AN UPDATED APPROACH TO THE PREDICTION OF DRYOUT AND VOID FRACTION FOR RBWR BUNDLES

X. Zhao, K. Shirvan, Y. Wu and M.S. Kazimi
Department of Nuclear Science and Engineering
Massachusetts Institute of Technology
77 Massachusetts Avenue, Cambridge, MA 02139, USA
Email: xgzhao@mit.edu

ABSTRACT

Unlike a traditional square lattice BWR fuel bundle, the Resource-Renewable Boiling Water Reactor (RBWR) fuel bundle is a tight hexagonal lattice. The different geometry, combined with different operating conditions, demands a re-examination of the standard BWR thermal hydraulic models. For dryout, the previously recommended MIT correlation, which is based on the CISE-4 formulation, had large scatter when compared to experimental data in its validation database. In a new study, narrowing the range of hydraulic diameter and operating conditions and including critical heat flux (CHF) data for tubes and annuli were investigated. A new MIT correlation was derived but yielded very similar low MCPR (minimum critical power ratio) values as previously predicted for the RBWR designs. Another methodology, the 2006 CHF look-up table of Groeneveld was also used to predict dryout in RBWR type geometry. It was found that the effects of boiling length and axial power shape require further detailed investigation via higher fidelity simulations. For void fraction, experimental data and a three field model for annular flow regime revealed that the common drift flux approaches over-estimate the void fraction at smaller hydraulic diameters. The void fraction dependence on diameter below 10 mm requires further experimentation and high fidelity mechanistic simulations.

KEYWORDS
RBWR, tight lattice bundle, dryout, void fraction

1. INTRODUCTION

The Resource-Renewable Boiling Water Reactor (RBWR) proposed by Hitachi, Ltd. [1] is a promising future reactor based on industrially established light water reactor (LWR) technology. With the objective of providing actinide breeding and burning capabilities, an RBWR design differs from a typical BWR mainly in that its fuel bundle is a tight hexagonal lattice with heterogeneous axial fuel geometry. The different core geometry, combined with different operating conditions, demands a reevaluation of the standard BWR thermal hydraulic models. In addition, few experimental data of tight lattice bundles are available. Previous work at MIT [2] has focused on collecting dryout and void fraction databases for representative RBWR fuel bundle geometry and working conditions, and derived new best estimate models for both critical quality/power and void fraction.

The previously recommended MIT correlation for dryout prediction, which is based on the CISE-4 formulation, has shown large scatter when compared to experimental data in its validation range. Narrowing the ranges of pressures and mass fluxes to those similar to steady state operating conditions of RBWR-type designs greatly reduces the spread in the data. Additionally, critical power (CP) experimental data for tubes and annuli are integrated in the database to better quantify the trends for different parameters (mass flux, diameter, etc.), and an improved CP correlation is proposed to effectively capture the round tube and

annulus data. Another methodology using the 2006 critical heat flux (CHF) look-up table [3], a normalized data bank designed for 8 mm vertical water-cooled tubes, is also applied to compare with tube results of both experiments and the new MIT correlation.

The thermal margins of RBWR cores to dryout, referred to as the Minimum Critical Power Ratio (MCPR), are evaluated using MIT correlations and the look-up table. Two core designs, RBWR-AC and RBWR-TB2, have their overall parameters shown in Table I and normalized axial power distributions presented in Figure 1.

Table I. Overall design parameters of RBWR-AC and RBWR-TB2 [4].

Item	RBWR-AC	RBWR-TB2
Thermal power [MWt]	3926	3926
Fuel rod diameter [cm]	1.005	0.72
Core height [m]	1.347	1.015
Number of fuel bundles	720	720
Number of rods per assembly	271	397
Coolant average flow rate [kt/h]	22	22
Core average pressure [MPa]	7.2	7.2
Inlet enthalpy [kJ/kg]	1250	1250
Assembly mass flux [kg/m^2-s]	896	573
Hydraulic/Heated Diameter [mm]	4.1/4.4	6.1/6.6
Core radial power peaking factor	1.3	1.2

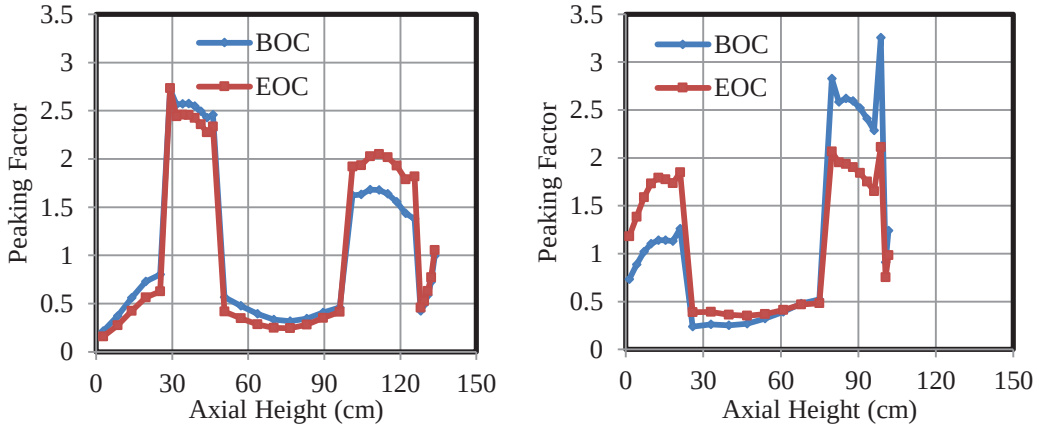

Figure 1. RBWR-AC (left) and RBWR-TB2 (right) relative axial power distribution[1] [5].

The previous comparison of void fraction data with 12 common empirical void fraction models indicated that at conditions similar to RBWR, the void fraction may be over-estimated by the common correlations [2]. In this study, a closer look at the correlation behavior revealed that the sensitive parameter is the smaller diameter and not the low mass flux of the RBWR designs. In fact, none of the commonly used empirical

[1] The large axial peaking factor near the exit is due to reflection of neutrons from the upper blanket zone. The RBWR-AC design employs a non-uniform fissile distribution to minimize this peaking.

void fraction correlations range of validity covers hydraulic diameters below 10 mm. More mechanistic approaches are needed in order to provide insight in the behavior of void fraction as a function of diameter in the range of RBWR design. Even with advancements in computational fluid dynamics, experimental data are required to properly measure the void fraction in heated tubes of small diameter.

2. DRYOUT PREDICTION ASSESSMENT

The prediction of critical power in tight lattice bundle geometries has proven to be challenging due to inability to predict all available databases with reasonable accuracy. Thus far, mainly 1-D lumped modeling of the experiments has been performed, where calculations are based on global parameters. The 1-D approach is simplified and easily implementable in core simulators. This section of work attempts to utilize such 1-D approach and extend its validation database to tubes and annuli.

2.1. Previous MIT Correlation Assessment

First, let us verify whether or not the previous MIT correlation [2] (also called M-CISE1 in this paper) is capable of providing an accurate prediction of the critical power for all the three types of heated geometries: tubes, annuli and tight lattice bundles.

2.1.1. Tube Data Comparison

The Thompson and Macbeth tube dryout database is used to compare the predicted critical power using M-CISE1 to the experimental data. Tests were performed at a variety of tube diameters and operating conditions. In order to be compatible with the RBWR design specifications, a total of 554 burnout data points are selected, and the range of parameters is summarized in Table II.

Table II. Dryout experiment test parameters for tubes.

Test	Axial Heating	Number of data	Pressure [MPa]	Mass flux [kg/m^2-s]	Diameter [mm]	Heated length [m]
Thompson & Macbeth [6]	Uniform	554	0.4 - 9	101 - 1,980	3 - 7.8	0.15 - 3.12

The average predicted/experimental critical power (PECP) of 0.85 was calculated, with a standard deviation (STD) of 0.14. In other words, the M-CISE1 correlation under-estimates the tube data by 15%. It was found that M-CISE1 is not able to predict tube CP accurately neither at very low pressure (over-estimation below 1 MPa) nor at pressures higher than 3.5 MPa (under-estimation). It is noted that the original CISE-4 formulation was based on pressure ranges between 5-7 MPa. The PECPs are generally under-estimated at mass fluxes above 1,000 kg/m^2-s and for boiling lengths smaller than 1.5 m. The trend of increasing PECP as boiling length increases was observed. The M-CISE1 correlation was also unable to effectively capture the dependence on diameter when larger than 4.5 mm.

2.1.2. Annulus Data Comparison

Four reference databases were used for the evaluation of CP in internally heated annuli, as presented in Table III. Experimental data indicate that the thermal performance of the annulus was unaffected by the alternate high and low heat flux profile or the presence of a hot patch compared to a uniform power distribution, within the selected ranges of parameters. In the last reference (Janssen & Kervinen), a single rod is uniformly heated in annular geometry with ranges of parameters quite different from those in the

other references. The major disparity occurs due to a significantly larger hydraulic diameter, which is well beyond the RBWR designs.

Table III. Dryout experiment test parameters for annuli.

Test	Axial heating	Number of data	Pressure [MPa]	Mass flux [kg/m^2-s]	Hydraulic diameter [mm]	Heated diameter [mm]	Heated length [m]	Axial peaking factor
1 - Beus & Seebold [7]	Uniform	22	5.5 - 11	336 - 1,363	5.6	15.2	2.13	1
	Alternate	11						1.27
	Alternate with hot patch	9						2.19
2 - Beus & Humphreys [8]	Alternate	19	5.5 - 11	290 - 1,248	5.5	14.8	2.13	1.76
	Alternate with hot patch	15						2.7
3 - Mortimore & Beus [9]	Uniform	15	8.3 - 11	332 - 1,396	5	13.3	2.13	1
	Hot patch of 1.5 heat flux ratio	12						1.5
	Hot patch of 2.25 heat flux ratio	14						2.25
4 - Janssen & Kervinen [10]	Uniform	282	4.1 - 10.2	354 - 1,980	8.5	22.3; 24.6	1.8 - 2.7	1

The average PECP of 0.83 with a STD of 0.09 was calculated. Though the average PECP is slightly lower than that of tube data, the STD is significantly less. It was noticed that the effect of pressure on PECP is minimal, though, no low pressure data was available. Similarly, the hydraulic over heated diameter parameter did not have a significant influence on PECP. A slightly increasing tendency of PECP with increasing mass flux was observed, whereas it decreased when hydraulic diameter or boiling length was larger. Interestingly, the trend observed in PECP of annuli data as a function of boiling length was opposite of that of tubes.

2.1.3. Bundle Data Comparison

Table IV. Dryout experiment test parameters for tight lattice bundles.

Test	Number of rods	Axial heating	Number of data	Pressure [MPa]	Mass flux [kg/m^2-s]	Hydraulic diameter [mm]	Heated diameter [mm]	Heated length [m]	Axial peaking factor
JAEA-A [11]	7	Uniform	98	1 - 8.5	73 - 2,000	2.35	3.56	1.8	1
JAEA-B [12]	7	Double-humped	96	1 - 8.5	300 - 1,381	2.86	4.34	1.26	2.2
JAEA-C [13]	37	Double-humped	117	2 - 9	206 - 1,005	4.42	5.32	1.26	2.23
JAEA-D [13]	37	Double-humped	148	2 - 9	300 - 1,500	3.71	4.44	1.26	2.23
Toshiba-1 [14]	7	Stepped cosine	6	7	472 - 1,744	4.85	7.29	1.6	1.2
Toshiba-2 [14]	7	Stepped cosine	13	7	489 - 1,961	5.91	9.03	0.8; 1.6	1.2
Toshiba-3 [14]	7	Stepped cosine	6	7	600 - 1,711	7.03	10.95	1.6	1.2
Toshiba-4 [14]	14	Stepped cosine	21	1 - 8	385 - 1,396	5.74	9.55	1.6	1.2

The tight lattice bundle test parameters used as validation database for the previous MIT correlation are listed in Table IV. The results of tight lattice bundle CP prediction by M-CISE1 are reported in [2] and replicated here for the purpose of improving the correlation and more detailed investigation of its performance. As reported in [2], M-CISE1 gives a mean PECP of 1.00 (with a STD of 0.17). More discussion on specific trends observed in the experimental data is given in Section 2.2.

2.2. New MIT Correlation Development and Assessment

As shown in Section 2.1, M-CISE1 significantly under-predicts tube and annulus data, by 15% and 17%, respectively. Since the previous correlation cannot cover CP prediction of all the three types of heated geometry, an updated version is necessary to improve its performance.

The methodology of the new M-CISE (also named M-CISE2) development is as follows:

- Adjust the correlation and make it match tube data as closely as possible;
- Adjust the correlation and make it match annulus data as closely as possible (the $\frac{D_e}{D_h}$ factor is introduced in this step);
- Introduce the R_f factor (constant) and adjust the correlation to fit bundle data (mean PECP = 1.00).

The effect of axial peaking is not accounted for the correlation, because annuli experiments with non-uniform heating up to 2.7 times the average do not show any significant impact on critical power. The radial pin peaking factor (R_f) is considered to be constant in the new correlation, since the considered data sources for bundles that are relevant to RBWR designs show no strong dependence on R_f. This is somewhat inconsistent with data for regular BWR bundles, where there is stronger dependence on R_f. Furthermore, the exact local flow distribution remains unknown with the 1-D analysis approach, which limits the use of a geometry dependent radial peaking factor as used by [14]. The value of R_f is set as 1.1 to better match the bundle data.

The updated M-CISE correlation is presented in Eq. (1). The range of experimental data used for comparison is listed in Table V.

$$X_{cr} = \left(\frac{D_e}{D_h}\right)^{0.83} \left(\frac{a\, L_b}{b + L_b}\right) R_f^{-1} \tag{1}$$

Where:

$$b = 0.279 \left(\frac{P_c}{P} - 1\right)^{0.4} G\, D_e^{1.4}$$

If $G \le G^*$ then:

$$a = \left(1 + 1.481\times10^{-4} \left(1 - \frac{P}{P_c}\right)^{-3} G\right)^{-1}$$

Otherwise:

$$a = \left(1 - \frac{P}{P_c}\right) / (G / 1000)^{1/3}$$

with:

$$G^* = 3375 \left(1 - \frac{P}{P_c}\right)^3,\ P_c = 22.064 \text{ MPa},\ R_f = 1.1 \text{ for bundles}$$

D_e, D_h and L_b in m, P in MPa, G and G^* in kg/m^2-s.

The mean and STD values for the predicted/experimental critical power with M-CISE1 and M-CISE2 for all of the three heated geometries (tubes, annuli and tight lattice bundles) are summarized in Table VI,

which divides the data set for the complete pressure range and the nominal operating pressure of an RBWR (7 ± 0.5 MPa).

Table V. Parameter ranges for the M-CISE2 correlation.

Parameter	Low	High
Pressure [MPa]	0.4	11
Mass Flux [kg/m^2-s]	73	2,000
Hydraulic Diameter [mm]	2.35	8.5
Heated Diameter [mm]	3	24.6
Heated Length [m]	0.15	3.12

Table VI. PECP mean and standard deviation (STD) values for tube, annulus and bundle data.

Correlation		M-CISE1				M-CISE2			
Pressure range		All		7 ± 0.5 MPa		All		7 ± 0.5 MPa	
Test		Mean	STD	Mean	STD	Mean	STD	Mean	STD
Tubes		0.85	0.14	0.69	0.09	0.90	0.13	0.74	0.08
Annuli		0.83	0.09	0.81	0.07	0.90	0.09	0.89	0.08
Bundles	JAEA-A	0.71	0.07	0.68	0.03	0.69	0.09	0.65	0.03
	JAEA-B	1.04	0.08	1.04	0.08	1.04	0.09	1.04	0.09
	JAEA-C	1.01	0.06	1.01	0.06	1.01	0.07	1.01	0.07
	JAEA-D	1.12	0.07	1.12	0.08	1.11	0.08	1.11	0.07
	Toshiba-1	1.18	0.07	1.18	0.07	1.20	0.10	1.20	0.10
	Toshiba-2	1.06	0.10	1.06	0.10	1.16	0.15	1.16	0.15
	Toshiba-3	0.84	0.04	0.84	0.04	0.89	0.02	0.89	0.02
	Toshiba-4	1.26	0.12	1.33	0.09	1.35	0.09	1.38	0.12
	All bundles	1.00	0.17	1.00	0.17	1.00	0.19	1.00	0.18

As can be noticed in Table VI, M-CISE2 under-predicts tube data by 5% less than the previous correlation, and the average PECP for annulus data is increased by 7% with the new correlation.

Among the three investigated geometries, the tube data has the fewest dependent parameters that could affect its CP, since neither radial peaking nor hydraulic/heated diameter ratio is applicable. However, Table VI shows that despite efforts made for improvement of the correlation, M-CISE cannot accurately predict tube CP, especially at nominal pressure (7 ± 0.5 MPa) where the under-estimation can reach up to more than 20%. This under-estimation could result from many possible reasons including the applicability of bundle formulation to tubes. Surprisingly, the comparison of the tube data at 7 MPa to the 2006 CHF look-

up table [3] also resulted in such inconsistency. The prediction of the annulus data has been improved mainly due to the modification of the scaling factor (hydraulic/heated diameter).

As for bundle data, both M-CISE1 and M-CISE2 are able to predict the overall bundle CP with an average of 1.0. The discrepancies between different test sections and even within some test sets are far from negligible, which lead to a larger STD in comparison to tube and annulus CP prediction. In the following sub-sections, effect of different parameters on critical power and PECP will be surveyed with the new M-CISE correlation (M-CISE2).

2.2.1. Effect of Pressure

It is generally well established that the CP increases at low pressure and reaches a maximum value at 3 to 5 MPa, before decreasing at high pressure. The dependence on relatively high pressure of CP and PECP is shown in Figure 2. For tube data, although not being significant, an increment of 3 MPa (from 4 to 7 MPa) in pressure gives rise to a drop of 11% in experimental CP, 17% in predicted CP and 4% in PECP. Similar trend is observed for annuli data, whilst the PECP becomes more pressure dependent for bundles: an increase of 3 MPa (from 3 to 6 MPa) leads to a reduction of experimental CP by 2% but a drop of PECP by about 15%. Since the pressure is only presented by a dimensionless parameter (P/P_c) in the original CISE-4 correlation and no changes have been made for M-CISE, further efforts are necessary to evaluate the pressure dependence of critical quality (and thus critical power), especially for bundles.

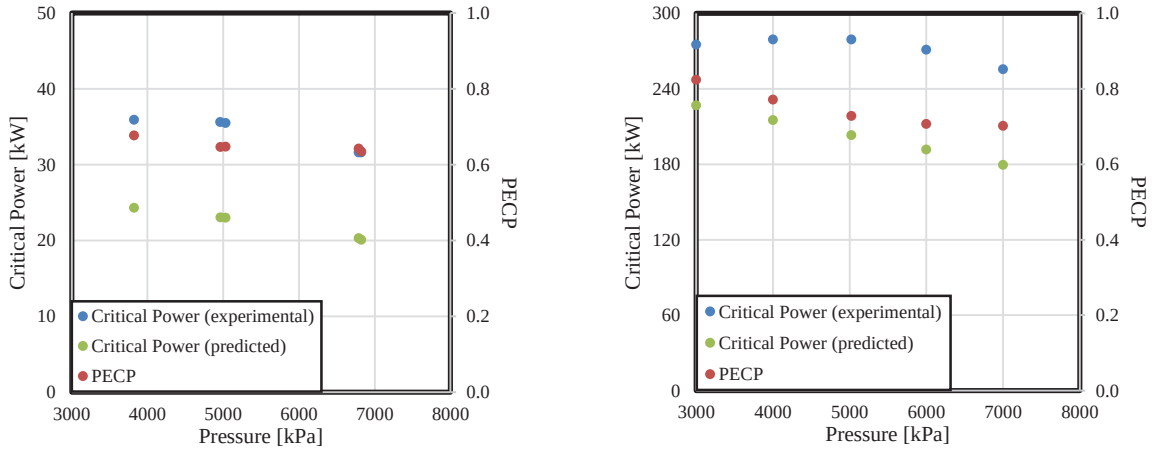

Figure 2. Pressure effect on CP and PECP: (left) Tube data [6] (G = 1,017 kg/m^2-s, D = 5.6 mm, L_b = 0.85 m); (right) JAEA-A bundle data [11] (G = 1,000 kg/m^2-s, D_e/D_h = 0.66, L_b = 1.72 m, R_f = 1.3).

2.2.2. Effect of Mass Flux and Bundle Geometry

As can be seen in Figure 3 (left), Toshiba-1 and -4 test sets show significant PECP rise when the mass flux increases whereas it stays flat for the Toshiba-2 and -3 (PECP predictions imply that the mass flux dependence is correctly predicted). As for JAEA-C and -D bundle tests (Figure 3 (right)), PECP value for JAEA-D rises up slightly to a peak at low mass flux (below 600 kg/m^2-s) before dropping down when G becomes higher. Due to the scatter in the experimental data, it is not clear whether the mass flux dependence in the JAEA-C data set is fully captured. In addition, one can conclude from Figure 3 that the remarkable discrepancies between different tests under the same working conditions are due to different bundle

geometries (tightness i.e. D_e/D_h, channel box shape, gap between rod and shroud). Such effects are only modeled by the D_e/D_h term in the M-CISE formulation.

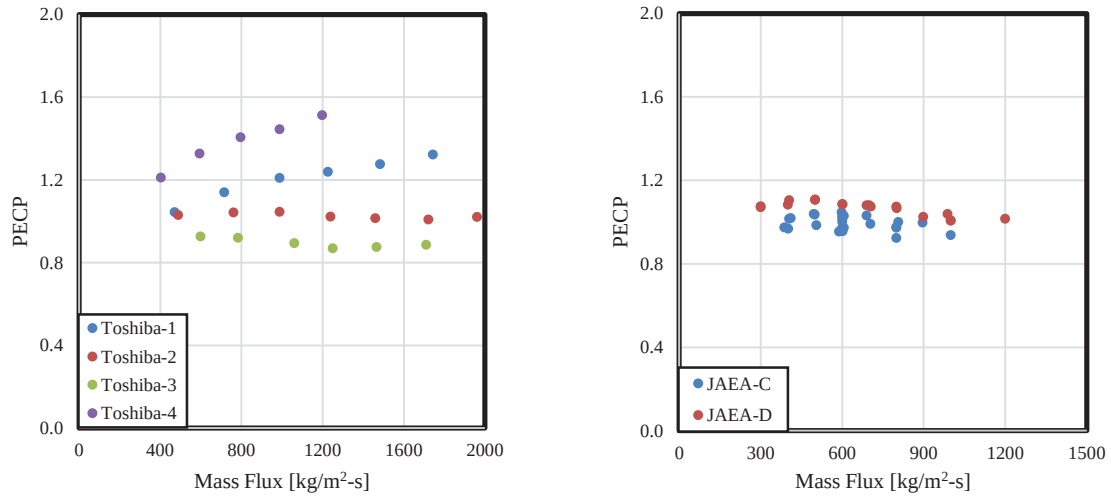

Figure 3. Mass flux and bundle geometry effect on PECP:
(left) Toshiba bundle data [14] (P = 7 MPa, D_e/D_h = 0.60-0.67, L_b = 1.31-1.45 m, R_f = 1.15-1.18);
(right) JAEA-C & -D bundle data [13] (P = 7.2 MPa, D_e/D_h = 0.83-0.84, L_b = 0.86-0.88 m, R_f = 1.0).

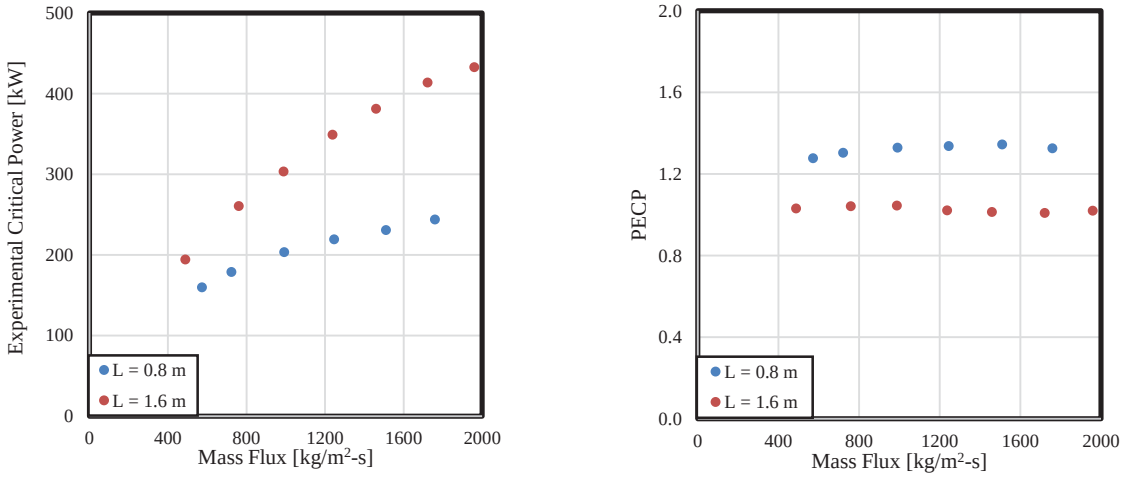

Figure 4. Heated length effect on CP and PECP: Toshiba-2 bundle data [14] (P = 7 MPa, D_e/D_h = 0.65, R_f = 1.18, L_b = 0.59-0.69 m for L = 0.8 m and 1.35-1.45 m for L = 1.6 m).
(left) Experimental CP vs. Mass flux; (right) PECP vs. Mass flux.

2.2.3. Effect of Heated Length

The 7-rod Toshiba-2 bundle test included the heated length effect on dryout, and the experimental results showed that critical power is strongly dependent on the heated length (or the boiling length). As can be seen in Figure 4 (left), each data set has a different dependence on mass flux. Figure 4 (right) shows the PECP

of the two data sets. One can conclude that when the heated length is doubled (from 0.8 to 1.6 m), the PECP rises by about 30%, from 1.03 to 1.32 (average over the mass flux range assuming no obvious dependence upon it, which is an appropriate estimation considering Figure 3). However, this sensitivity was not observed for tube and annuli data. This result implies that for bundles, the higher sensitivity of critical power to boiling length could be coupled to spacers as well as bundle intra-assembly coolant mixing. Unfortunately the JAEA experiments changed more than just the heated length and the effect of the boiling length cannot be investigated separately.

2.2.4. Effect of Axial Peaking Condition

A different axial power distribution may change the position of dryout and could affect the heat removal performance. However, as mentioned earlier in this section, the M-CISE2 correlation does not include any functions of axial peaking factor, because the annuli data displayed no significant impact of axial power factor on CP. The JAEA-B test [12] reported that under the same operating condition, the double-humped axial power shape gives lower CP compared to the uniform axial power shape (JAEA-A test), as displayed in Figure 5 (left). Figure 5 (right) shows that the average PECP over a range of mass fluxes is increased by 40% (from 0.65 to 1.05) when comparing JAEA-A (uniform) to -B (non-uniform) tests.

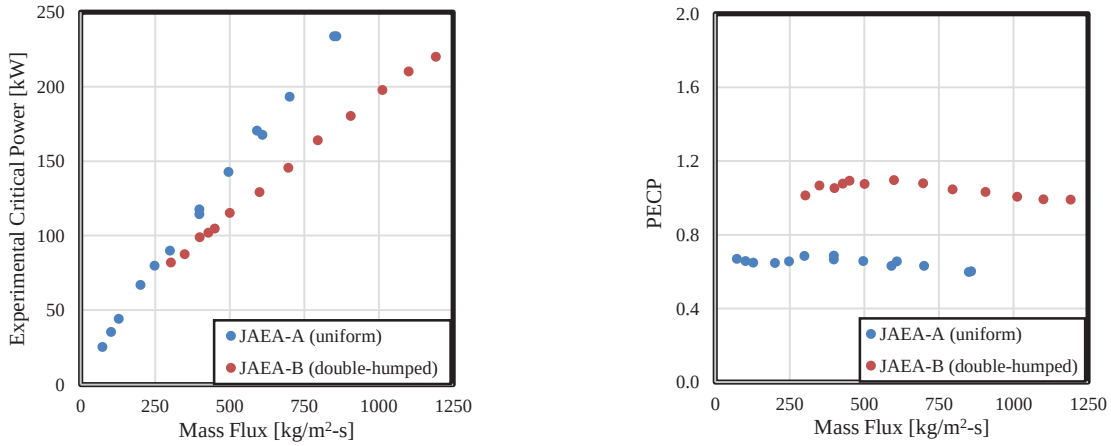

Figure 5. Axial peaking condition effect on CP and PECP: JAEA-A and -B bundle data [11][12] (P = 7.2 MPa, D_e/D_h = 0.66, inlet subcooling = 5 K, R_f = 1.3 for JAEA-A and 1.4 for JAEA-B, L = 1.8 m for JAEA-A and 1.26 m for JAEA-B). (left) Experimental CP vs. Mass flux; (right) PECP vs. Mass flux.

However, one cannot conclude from the results presented in Figure 5 (right) that the lower critical power for the non-uniform heating channel is due only to the axial peaking factor present in JAEA-B tests. In fact, multiple parameters come into play in this comparison (heated/boiling length, bundle geometry, radial peaking, axial power shape), and any of them could contribute to this under-prediction of PECP. For instance, JAEA-A bundle is 43% longer than -B bundle, which, as discussed in Section 2.2.3, doubling the heated length resulted in 30% difference in the prediction of PECP for the Toshiba experiments. The double-humped power shape for JAEA-B test shows a downward heating region at the location of the second hump, and it is known that CP typically occurs at a location of downward heated region, downstream of a spacer grid [15]. Unfortunately, the non-uniform heating annuli data were performed with only upward heated test sections. In general, the effect of axial power profile on dryout at BWR type conditions has been shown to be on the order of 5-20% by various studies [16][17][18]. The higher axial peaking toward the outlet has

shown to degrade the critical power compared to a uniform power distribution, though, the magnitude of the change is unclear. In fact, the magnitude of impact has been shown to depend on the geometry and spacer grid configuration [19]. Additionally, due to the presence of high peaking factors in the lower region of the RBWR designs, at the beginning of the first fissile zone, some consideration on the limit of local heat flux before and after the onset of annular flow is required [20].

2.2.5. Narrowing range of Bundle Data

As we narrow the ranges of pressure and mass flux of the bundle data listed in Table IV to those similar to steady state operating conditions of RBWR-type designs, the STD is significantly reduced to 0.09. Specifically, if the mass flux and hydraulic diameter are limited to 500-1500 kg/m^2-s and 2.8-7.5 mm, respectively, at 7±0.5 MPa operating pressure, then the mean PECP using the previous M-CISE correlation was calculated to be 0.95. In order to reach a mean PECP of 1.00, starting with the M-CISE1 formulation from [2], the multiplier in front of mass flux in the "a" term was changed from 0.7 to 0.4 and the diameter dependence in the "b" term was changed from power of 1.2 to 1.1. This updated correlation will be referred to as the N-CISE (Narrow M-CISE) in the following section.

2.3. MCPR Evaluation of RBWR-AC and RBWR-TB2

This section evaluates the Minimum Critical Power Ratio (MCPR) of the RBWR-AC and TB2 designs using MIT correlations (previous, narrow and new) as well as the look-up table. The methodology applied in the look-up table approach is described in [21] except that: (1) the dryout crisis is not assumed to occur at the exit of the hot bundle, but at the end of the upper fissile zone; (2) the same bundle geometry factor as in the M-CISE2 formulation is taken into account.

Table VII. Critical quality (X_{cr}) and MCPR evaluation of RBWR-AC and RBWR-TB2.

Core	RBWR-AC				RBWR-TB2			
Flow rate	Nominal		120%		Nominal		120%	
Correlation	X_{cr}	MCPR	X_{cr}	MCPR	X_{cr}	MCPR	X_{cr}	MCPR
M-CISE2	0.52	1.01	0.48	1.11	0.57	1.15	0.53	1.28
M-CISE1	0.55	1.06	0.50	1.15	0.58	1.16	0.53	1.28
N-CISE	0.52	1.01	0.47	1.09	0.53	1.06	0.48	1.17
Look-up table	0.71	1.35	0.63	1.43	0.59	1.19	0.55	1.34

As listed in Table VII, the predicted critical quality and MCPR values by the M-CISE1 and M-CISE2 correlations are very close, especially for the RBWR-TB2 design. The look-up table method predicts much higher results for RBWR-AC compared to MIT correlations, but predicts similar values for TB2, since it uses the local heat flux values. As shown in Figure 1, RBWR-TB2 maximum axial peaking factor is over twice as much as that of AC. The N-CISE results in more conservative prediction with a smaller STD. An improvement of 8-15% can be observed with 20% increase in the core flow rate. However, in all cases except for RBWR-AC using look-up table, the typical BWR MCPR steady state design limit of 1.3 is not achieved by either design. Depending on the accuracy of the correlation, this conclusion remains tentative.

3. VOID FRACTION PREDICTION ASSESSMENT

The limited JAEA 37 rod bundle experimental data with water at both 7 and 2 MPa, shown in Figure 6, for annular flow regime imply that, at lower mass flux (600-800 kg/m^2-s) and smaller hydraulic diameter compared to a conventional BWR assembly, the void fraction is over-estimated using traditional void quality relations, such as the Chexal-Lellouche correlation used in system codes such as RELAP5 [2]. This trend is supported by low flow experimental data with water at low pressures (atmospheric) for the NEPTUN tight lattice bundle experimental facility designed with a hydraulic diameter of 4 mm [2]. An additional study by Triplett et al. [22] compared the Chexal-Lellouche correlation predictions to experimental measurement of void fraction with air and water for 1-1.5 mm diameter tubes at atmospheric pressure and a similar trend was observed in the annular flow regime. This over-prediction suggests that the interfacial momentum transfer in low flow and small hydraulic diameters is significantly different from large hydraulic diameters. In all available experimental databases, the LPG correlation (noted Liao in Figure 6) predicted void fraction that resulted in closest agreement with the experimental data [2].

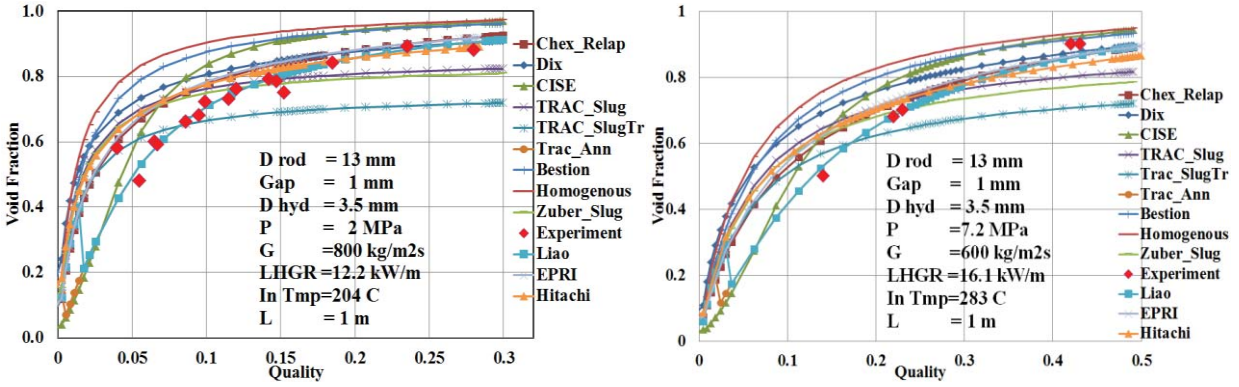

Figure 6. Axial void fraction for the JAEA 37-rod bundle type at (left) 2 MPa and (right) 7 MPa (figure from Shirvan et al. [2]).

Figure 7 shows the sensitivity of the RELAP5 and LPG void fraction correlations at 10% and 25% quality for the RBWR-AC conditions outlined in Table I. As shown in Figure 7, at 10% quality, the calculated void fraction by LPG is under-estimated by ~15%, while at high qualities, the void fraction prediction is similar to the RELAP5 correlation. Figure 7 (left) shows no significant difference in dependence on mass flux, while Figure 7 (right) shows significant dependence on hydraulic diameter, in fact, opposite dependence. Neither correlation validation database covers hydraulic diameters smaller than 10 mm [23]. Interestingly, the LPG correlation predicts far lower than expected void fraction at hydraulic diameters of a typical BWR. Therefore, it is only a coincidence that the LPG correlation agrees well will the small available experimental data base on void fraction in small hydraulic diameters.

The NUPEC BWR Full-size Fine-mesh Bundle Tests (BFBT) including PWR subchannel tests are perhaps the best available data to verify void-quality relations in BWR bundles. These tests are part of an NEA/NRC international benchmark (for more information OECD/NEA website can be referred). Unfortunately, the BFBT hydraulic diameter is larger than 1 cm, which is well outside the range of RBWR designs. Nevertheless, high fidelity numerical simulations of NUPEC tests have been performed under Computational Fluid Dynamics (CFD) two phase Eulerian framework [23-27]. In all studies, the accuracy of the models were within 15% void fraction compared to experimental results, and the models were highly sensitive to the many closures required in the two-phase Eulerian framework. In addition, all the typical closures that were used in simulation of NUPEC tests are susceptible to numerical instabilities under high

local heat fluxes [28], which is a characteristic of RBWR type design. Thus, the use of CFD was deemed to be currently immature to correctly capture the diameter dependence on void fraction predictions.

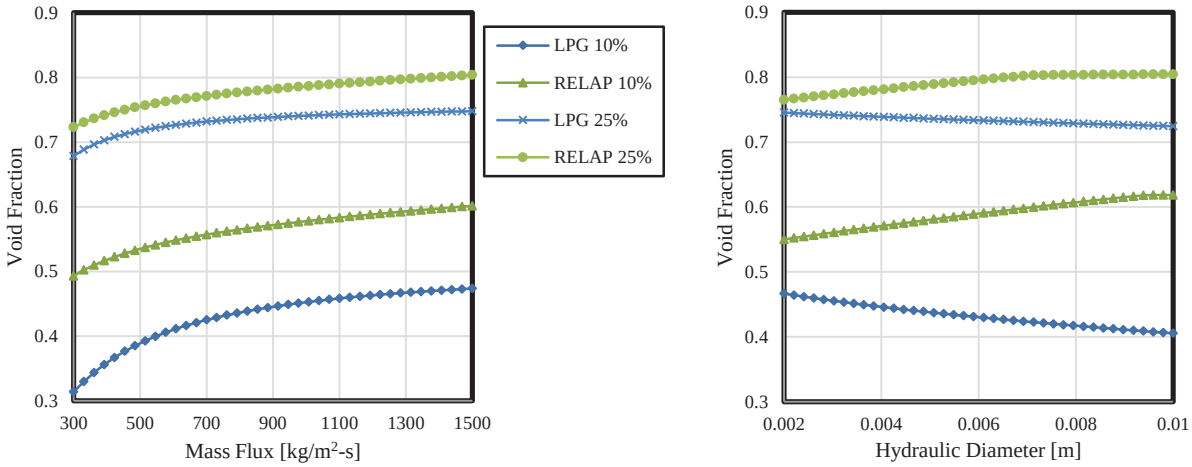

Figure 7. Sensitivity of void fraction prediction to (left) mass flux at RBWR-AC hydraulic diameter and to (right) hydraulic diameter at RBWR-AC mass flux for the LPG and RELAP correlations at 10 and 25% quality for 7 MPa.

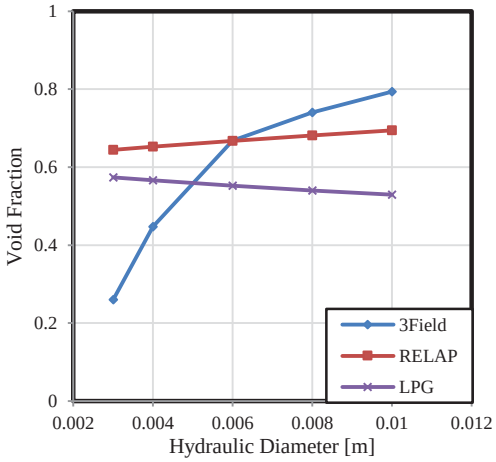

Figure 8. Three field model vs. RELAP5 and LPG correlations at 15% quality.

The other mechanistic approach is using a three field model (liquid film, entrained droplets and vapor) to describe the annular flow regime, where some recent success has been shown in prediction of dryout for both tubes [29] and bundles [30]. Similar model was coded as described in [30] except that the criteria for onset of annular flow regime was assumed to be $J_g^* = 1$, as recommended by Hewitt [31], where J^* is the non-dimensional superficial velocity. The models take advantage of tracking the liquid film thickness and therefore able to provide an upper bound for void fraction. It is important to note that similar to the CFD framework, the three field framework also requires many closures that are currently empirically based. As shown in Figure 8, the three field model alludes that the void fraction should decrease more sharply than predicted by the RELAP5 correlation. While the predicted trend on diameter dependence of void fraction

could be supported by experimental data, the utilized model severely under predicts void fraction at below 4 mm. Judging by Figure 7 and Figure 8, the LPG correlation should not be used for RBWR-TB2 design analysis, since its hydraulic diameter is greater than 6 mm and the RELAP correlation will most likely give the more accurate prediction, pending further V&V.

4. CONCLUSIONS

The development of proper critical power and void fraction correlations for the RBWR designs is challenging. In this new study, the previous bundle data were supplemented with relevant CHF data for tubes and annuli to better quantify the trends for different thermal hydraulic parameters. The new M-CISE correlation still yielded a similar low MCPR prediction (less than 1.3) as the previously recommended M-CISE correlation. The 2006 look-up table was shown to overestimate CP compared to the CISE based correlations. The dependence on boiling length and the role of RBWR double-humped axial power shape are still not clear and interpretations of the available data will be investigated via subchannel analysis and higher fidelity simulation in the future. For void fraction predictions, experimental data along with three field numerical simulation of annular flow in small hydraulic diameters have revealed that the current empirical models are unable to properly model the effects of diameter on void fraction predictions at qualities less than 25%. Future experiments and higher fidelity simulations will be performed to investigate the dependence of void fraction on hydraulic diameter in the range of interest. Specifically, sensitivity studies on the closure terms in the utilized three field model will be performed.

ACKNOWLEDGMENT

This work was partially funded by Hitachi Research Laboratory, Hitachi, Ltd.

REFERENCES

1. R. Takeda, M. Aoyama, M. Moriwaki, S. Uchikawa, O. Yokomizo and K. Ochiai. General Features of Resource-Renewable BWR (RBWR) and Scenario of Long-term Energy Supply. *Proc. of International Conference on Evaluation of Emerging Nuclear Fuel Cycle Systems*, p. 938 (1995).
2. K. Shirvan, N. Andrews and M.S. Kazimi. Best Estimate Void Fraction and Critical Power Correlations for Tight Lattice BWR Bundles. *Proc. of ICAPP 2013*, paper no. FA159 (2013).
3. D.C. Groeneveld, J.Q. Shan, A.Z. Vasic, L.K.H. Leung, A. Durmayaz, J. Yang, S.C. Cheng and A. Tanase. The 2006 CHF Look-up Table. *Nuclear Engineering and Design*, **237**, 1909-1922 (2007).
4. K. Shirvan and M.S. Kazimi. Reduced Moderated Boiling Water Reactor Thermal Hydraulics and Safety Assessment. Hitachi Technical Report (2015).
5. T. Downar et al.. Analysis of RBWR AC and TB2 design with SERPENT/PARCS/PATHS code system. Hitachi Final Report (2015).
6. B. Thompson and R.V. Macbeth. Boiling Water Heat Transfer Burnout in Uniformly Heated Round Tubes: a Compilation of World Data with Accurate Correlations. United Kingdom Atomic Energy Authority, AEEW-R356 (1964).
7. S.G. Beus and O.P. Seebold. Critical Heat Flux Experiments in an Internally Heated Annulus with a Non-Uniform, Alternate High and Low Axial Heat Flux Distribution (AWBA Development Program). DOE Research and Development Report, WAPD-TM-1475 (1981).
8. S.G. Beus and D.A. Humphreys. Critical Heat Flux Tests with High Pressure Water in an Internally Heated Annulus with Alternating Axial Heat Flux Distribution (AWBA Development Program). DOE Research and Development Report, WAPD-TM-1451 (1979).
9. E.P. Mortimore and S.G. Beus. Critical Heat Flux Experiments with a Local Hot Patch in an Internally Heated Annulus (LWBR Development Program). DOE Research and Development Report, WAPD-TM-1419 (1979).

10. E. Janssen and J.A. Kervinen. Burnout Conditions for Single Rod in Annular Geometry, Water at 600 to 1400 Psia. Atomic Power Equipment Department, General Electric Company, GEAP-3899 (1963).
11. M. Kureta and H. Akimoto. Critical Power Correlation for Axially Uniformly Heated Tight-Lattice Bundles. *Nuclear Technology*, **143**, 89-100 (2003).
12. W. Liu, M. Kureta and H. Akimoto. Critical Power in 7-Rod Tight Lattice Bundle. *JSME International Journal*, **47**, No. 2, 299-305 (2004).
13. W. Liu, M. Kureta, H. Yoshida, A. Ohnuki and H. Akimoto. An Improved Critical Power Correlation for Tight-Lattice Rod Bundles. *Journal of Nuclear Science and Technology*, **44**, No. 4, 558-571 (2007).
14. T. Yamamoto, M. Akiba, S. Morooka, K. Shirakawa and N. Abe. Thermal Hydraulic Performance of Tight Lattice Bundle. *JSME International Journal*, **49**, No. 2, 334-342 (2006).
15. Z. Stosic. Study on Thermal Performance and Margins of BWR Fuel Elements. *Proc. of ICONE-7*, 7283 (1999).
16. J. Yang, D.C. Groeneveld, L.K.H. Leung, S.C. Cheng and M.A. El Nakla. An Experimental and Analytical Study of the Effect of Axial Power Profile on CHF. *Nuclear Engineering and Design*, **236**, 1384-1395 (2006).
17. C. Adamsson and H. Anglart. Influence of Axial Power Distribution on Dryout: Film-flow Models and Experiments. *Nuclear Engineering and Design*, **240**, 1495-1505 (2010).
18. N.E. Todreas and W.M. Rohsenow. The Effect of Non-uniform Axial Heat Flux Distribution on the Critical Heat Flux. MIT, Report No. 9843-37 (1965).
19. H. Anglart. Study of the Influence of Axial Power Distribution on Dryout. *Proc. of ICONE-18*, 29050 (2012).
20. J.P. Manning, S.P. Walker and G.F. Hewitt. A Lower Bound for the Dryout Quality in Annular Flow. *Proc. of ICONE-22*, 30877 (2014).
21. N.I. Kolev. Check of the 2005-Look-up Table for Prediction of CHF in Bundles. *Nuclear Engineering and Design*, **237**, 978-981 (2007).
22. K.A. Triplett et al.. Gas-liquid Two-phase Flow in Microchannels: Part II: Void Fraction and Pressure Drop. *Int. J. of Multiphase Flow*, **25**(3), 395-410 (1999).
23. P. Coddington and R. Macian. A Study of the Performance of Void Fraction Correlations Used in the Context of Drift-flux Two-phase Flow Models. *Nuclear Engineering and Design*, **215** (2002).
24. W.K In et al.. CFD Simulation of the NUPEC BWR Full-size Fine-mesh Bundle Test for a Void Distribution Benchmark. *Proc. of KNS Spring Meeting*, **40** (2009).
25. E. Krepper and R. Rzehak. CFD Analysis of a Void Distribution Benchmark of the NUPEC PSBT Tests: Model Calibration and Influence of Turbulence Modelling. *Science and Technology of Nuclear Installations*, **2012**, 10 (2012).
26. K. Goodheart *et* al.. Analysis of the Interfacial Area Transport Model for Industrial 2-phase Boiling Flow Applications. *NURETH-15*, Pisa, Italy, 067 (2013).
27. A. Tentner *et* al.. Development and Validation of a Computational Fluid Dynamics Model for the Simulation of Two-phase Flow Phenomena in a Boiling Water Reactor Fuel Assembly. *Proc. of 17th Int. Conf. on Nuclear Engineering*, Brussels, Belgium, 75135 (2009).
28. K. Shirvan *et* al.. Assessment of a Baseline Two Phase CFD Closure for PWR Applications. *Transactions of the American Nuclear Society*, Washington D.C. (2013).
29. T. Okawa, A. Kotani, I. Kataoka and M. Naito. Prediction of Critical Heat Flux in Annular Flow Using a Film Flow Model. *Journal of Nuclear Science and Technology*, **40**, 388 (2003).
30. C. Adamasson and J.M. Le Corre. Modeling and Validation of a Mechanistic Tool (MEFISTO) for the Prediction of Critical Power in BWR Fuel Assemblies. *Nuclear Engineering and Design*, **241**, 2843-2858 (2011).
31. G.F. Hewitt and A.H. Govan. Phenomenological Modelling of Non-equilibrium Flows with Phase Change. *Int. J. Heat Mass Transfer*, **33**, 229–242 (1990).